Anisotropy of the photo-elastic effect in Nd:KGd(WO_4)$_2$ laser crystals

P A Loiko[1]*, V G Savitski[2], A Kemp[2], A A Pavlyuk[3], N V Kuleshov[1] and K V Yumashev[1]

[1]Center for Optical Materials and Technologies, Belarusian National Technical University, 65/17 Nezavisimosti Ave., Minsk, Belarus 220013

[2]Institute of Photonics, University of Strathclyde, Wolfson Centre, 106 Rottenrow, Glasgow G4 0NW, United Kingdom, e-mail: vasili.savitski@strath.ac.uk

[3]A.V. Nikolaev Institute of Inorganic Chemistry, Siberian Branch of Russian Academy of Sciences, 3 Lavrentyev Ave., Novosibirsk, Russia 630090

*E-mail: kinetic@tut.by

Abstract. The anisotropy of thermal lensing and the photo-elastic effect is characterized for diode-pumped Nd:KGd(WO_4)$_2$ crystals cut along the N_p and N_g optical indicatrix axes and along its optical axis, $O = N_g+43°$, at a laser wavelength of 1067 nm. Distortions in the spatial profile of output laser beam are analyzed. The thermal lens is astigmatic; the orientation of its principal meridional planes, A and B, is determined by the anisotropy of photo-elastic effect. The thermal lens has opposite signs for rays lying in the principal meridional planes for N_p- and O-cut crystals; and it is positive for an N_g-cut crystal. The increase of thermal lens optical power after absorption of 1 W of pump power, i.e. the thermal lens sensitivity factors $M_{A(B)}$, and astigmatism degree $S = |M_A–M_B|$ are determined. The photo-elastic effect was found to increase the optical power of thermal lens and was significant for all studied crystal orientations.

Keywords: double tungstates, diode-pumping, thermal lensing, photoelastic effect

PACS: 81.05.Xj; 78.20.N-; 65.40.De; 42.70.Hj

Short title: Anisotropy of photoelastic effect in Nd:KGd(WO_4)$_2$

1. Introduction

Nd- and Yb- doped potassium gadolinium tungstate, Nd:KGd$(WO_4)_2$ (KGW), is an attractive material for cw [1-4] and pulsed [5-8] low-threshold diode-pumped lasers operating in the vicinity of 1 and 1.3 μm. KGW is a biaxial crystal, with three crystal orientations having been employed so far for laser engineering: along the ***b*** (N_p) axis [1-3, 5-8], along the N_g axis [9-12] and along the optical axis (*O*) [13, 14], i.e. N_g+43° in the N_p-N_g plane [15]. Strong astigmatism of the thermo-optical properties of the material results in significant variation in the sign and value of the thermal lens in crystals cut for light propagation along the N_p and N_g axes under diode- or flash-lamp pumping [9, 12, 15, 16]. Thermal lens measurements were reported previously for the N_p and N_g-cut Nd:KGW crystals at the wavelength of 1.06 μm under the flash-lamp-pumping [9, 15, 16] and at the wavelength of 1.35 μm under the diode -pumping [12].

O-cut KGW laser crystals have recently attracted significant attention due to the so-called "conical refraction" effect [17]. This effect is thought to be responsible for polarization-tuning of the laser emission [13], and the "excellent" laser beam quality [14] in Nd:KGW lasers using this crystal cut. However, to the best of our knowledge, thermo-optical properties of the *O*-cut KGW crystal have never been taken into account when analyzing conical refraction effects in these lasers.

In this paper we present for the first time the results of experimental and theoretical analysis of thermal lens in the diode-pumped Nd:KGW laser with the crystal cut for light propagation along the optical axis (the so-called "conical refraction laser"). A direct comparison of thermal lens properties under the identical experimental conditions is made for Nd:KGW lasers with crystals cut along the N_p and N_g axes of optical indicatrix. It was found that, as has been reported in Nd:YLF [18], the photo-elastic effect and its anisotropy in KGW affects the sign and value of the thermal lens in the crystal. The contribution of the photo-elastic effect to the thermal lens at 1 μm was calculated for three orientations of the Nd:KGW crystal.

2. Experimental

KGW crystals with Nd ions concentration of 3 at. % were grown by the technique described in [19]. Three different crystal orientations were studied, namely N_p-, N_g- and *O*-cut (figure 1). The crystal thickness was 1 mm and the aperture was 3×3 mm^2.

The thermal lens in diode-pumped Nd:KGW laser crystals was characterized by analyzing changes in the spatial profile of the output laser beam (figure 2). For cw pumping, a fiber-coupled AlGaAs laser diode producing unpolarised emission was used (λ_p = 810 nm, FWHM ~ 3 nm). Pump radiation was focused into the laser crystal by a pair of spherical lenses (collimating lens, CL, and focusing one, FL). The radius of the pump beam ω_p inside the crystals was measured to be 180 μm. Pump absorption in all the Nd:KGW crystals under study was measured directly using the pump laser diode emission to be more than 97%. The input and output faces of the crystals were anti-reflection (AR) coated for the pump and laser (1067 nm) wavelengths. The crystals were kept in thermal contact with a copper heat-sink by means of heat grease; its temperature was maintained at ~17°C.

The laser cavity was formed by a concave HR@1067 nm mirror (R = 50 mm, HT@810 nm) and a flat output coupler, OC (T = 0.5%@1067 nm). The air gap between the crystal and the HR mirror was 13 mm; the total cavity length was 47 mm. The radius of the TEM_{00} cavity mode in the laser crystals was calculated by the ABCD-method to be ~180 μm. The polarization of the output beam was naturally-selected by the anisotropy of the laser gain (it was $\boldsymbol{E} \parallel N_m$ for N_p- and N_g-cut crystals). For the *O*-cut crystal near the threshold, the orientation of the vector of polarisation was very sensitive to the pump power (the similar behaviour was observed previously in [13] for *O*-cut Yb- doped KGW). However, at higher pump levels the laser polarisation stabilized to $E \perp N_m$. The output beam was near-Gaussian with the $M^2 < 1.1$. This M^2 value was found to be unchanged within the pump powers used in the experiments. The spatial profile of the output beam at a distance of 11 cm from the OC was measured using a CCD-camera. The second moment diameter of the beam was measured.

Significant astigmatism of the thermal lens in KGW crystals was reported in [9, 12]. This means that the laser output beam is, in general, elliptical. That is why the measurements of the laser beam sizes were performed along the principal meridional planes A and B, i.e. planes which correspond to major and minor semi axes of these ellipses. The dependence of the radii of the laser beam $\omega_{A(B)}$ along directions A (B) on the absorbed pump power P_{abs} was measured. The optical power of the thermal lens $D_{A(B)}$ and the sensitivity factor, $M_{A(B)} = dD_{A(B)}/dP_{abs}$ can then be calculated from the laser resonator parameters by the ABCD method [12, 20]. The sensitivity factor shows the increase of the thermal lens optical power on absorption of 1 W of pump power. The difference $S = |M_A – M_B|$ is called the astigmatism degree (for a spherical thermal lens $S = 0$). The orientation of A and B planes, $M_{A(B)}$ and S values make the complete set of thermal lens parameters.

3. Results

Typical spatial profiles of the output beam of the Nd:KGW lasers captured with the CCD-camera are presented in figure 3. Here the upper and lower images correspond to the low and high values of absorbed pump power of $P_{abs} = 0.1$ and 0.5 W. The profiles are near-circular for low pump level (near the laser threshold). With increase of the pump power, the profiles become elliptical.

The measured dependencies of the output beam radii, $\omega_{A(B)}$, on the absorbed pump power, P_{abs}, are shown in figure 4. Here the points are the experimental data; curves are the results of modelling with the ABCD-method. For the N_p- and O-cut crystals, the thermal lens results in expansion of the laser beam along the A direction and in its compression in orthogonal B direction. In contrast, for the N_g-cut crystal the thermal lens leads to expansion of the laser beam along both A and B directions.

In general, the orientation of the A and B planes is not directly related with polarization of the laser emission. Indeed, for the N_p-cut crystal, the A (B) directions make the angle of ~30° with the N_m (N_g) axes; for the O-cut crystal, they make the angle ~25° with the N_m ($\perp N_m$) axes; and for the N_g-cut crystal, A || N_m and B || N_p. The scheme illustrating this difference is presented in figure 5 (circles and ellipses correspond to spatial profiles of output beam at low and high pump levels).

It was demonstrated recently that the orientation of principal meridional planes for the flashlamp-pumped Nd:KGdW crystal is determined by the anisotropy of the thermal expansion [15]. According to our data, this is also true for the diode-pumping. Indeed, maximum and minimum values of the thermal expansion coefficient in the N_m-N_g plane correspond to the X'_1 and X'_3 principal axes, with $N_m \wedge X'_1 = 32.1°$ [21]. This is in agreement with our data, $A \wedge N_m \sim 33°$. As a result, for the N_p-cut crystal, A || X'_1 and B || X'_3. For the O-cut crystal, directions with max and min thermal expansion are rotated by ~ 30 º-anticlockwise from the N_m ($\perp N_m$) axes which is again in agreement with our data. Maximum and minimum values of the thermal expansion coefficient in the N_m-N_p plane (N_g-cut crystal) correspond directly to N_m and N_p axes. This also agrees with the observed coincidence of A and B directions with N_m and N_p axes (figure 3).

The ratio of the radii of an elliptical Gaussian beam, ω_A/ω_B, is denoted as the beam ellipticity, see figure 4(d). It increases monotonically with the increase of the pump power. For the N_p- and O-cut crystals, the beam ellipticity reaches ~1.2 at $P_{abs} = 1$ W. The N_g-cut crystal allows one to obtain lower distortion of the output laser beam (as the corresponding value of the beam ellipticity is less than 1.1).

The calculated dependencies of the optical powers of the thermal lens in the two meridional planes, D_A and D_B, on the absorbed pump power are presented in figure 6(a)-(c). ABCD-modeling of the laser resonator used [figure 6(d)] indicates that expansion (compression) of the output laser beam corresponds to the positive (negative) thermal lens in Nd:KGW crystal. Moreover, the value of ω is more sensitive to a positive lens. Thus, for the N_p- and O-cut crystals, the thermal lens is positive (negative) for rays lying in the A (B) planes; and it is positive for rays lying in all meridional planes for the N_g-cut crystal. These findings are supported by the previous results reported for the N_p and N_g-cut Nd:KGW crystals under the flash-lamp- and diode-pumping [9, 12, 15, 16].

The slopes of the dependencies in figure 6(a)-(c) are called thermal lens sensitivity factors, $M_{A(B)} = dD_{A(B)}/dP_{abs}$. These values are summarized in table 1. The difference of principal sensitivity factors is denoted as astigmatism degree, $S = |M_A - M_B|$. For the N_p-cut and O-cut crystals, the values of S are close and equal to ~1.6 m^{-1}/W. In contrast, the N_g-cut crystal offers near 8-times reduced astigmatism, $S \sim 0.2$ m^{-1}/W.

4. Discussion

Formation of the thermal lens in solid-state lasers is determined by three main effects, namely (i) the temperature variation of refractive index dn/dT, (ii) the photo-elastic effect (dependence of refractive index on thermally-induced stress, P_{PE}) and (iii) the bulging of crystal end faces due to non-uniform thermal expansion Q_{dist} [22]. These contributions are summarized in the so-called "generalized" thermo-optic coefficient [23], $\Delta = dn/dT + P_{PE} + Q_{dist}$. For diode-pumping of bulk crystals (plane stress approximation), optical power of the thermal lens can be determined as [23]:

$$D = \frac{P_{abs}\eta_h}{2\pi\omega_p^2\kappa}\left(\frac{dn}{dT} + P_{PE} + Q_{dist}\right) \quad (1),$$

where η_h is the fractional head load (for Nd^{3+} ions, it is usually estimated as the quantum defect, $1-\lambda_p/\lambda_l$, where λ_p and λ_l are the pump and laser wavelengths, correspondingly); ω_p is the pump spot radius (top-hat profile); κ is the thermal conductivity. It should be noticed that in previous publications on the thermal lens in cubic $Y_3Al_5O_{12}$, the Q_{dist} term was evaluated as $(n-1)(1+\nu)\alpha$, where ν is the Poisson ratio, n is the refractive index, and α is the thermal expansion coefficient in the direction of light propagation [22]. However, for KGW crystal the tensor of elastic constants C_{ij} is highly anisotropic and does not satisfy basic relations for high-symmetry materials like $Y_3Al_5O_{12}$ (even in rough approximation) [24], that is why the bulging of crystal end faces is described in KGW as $Q_{dist} = (n-1)\alpha$. Thermal conductivity κ is a scalar quantity for isotropic materials. However, for crystals with low anisotropy of thermal conductivity like double tungstates, directionally-averaged value of κ can be used [23]. Under longitudinal diode-pumping, heat flow in the crystal is predominantly transverse. Thus, κ should be averaged over the plane perpendicular to the light propagation direction.

To the date, the thermal conductivity for $KGd(WO_4)_2$ has been measured only for a few directions in the crystal [25, 26]. Complete characterization of κ tensor has been performed for another representative of double tungstates, isostructural $KLu(WO_4)_2$ [27]. Since the thermal properties within this crystal family are very similar, we can use this data in the present paper. Directionally-averaged values of κ for N_p-, O- and N_g-cut crystals are summarized in the table 2.

The so-called thermal coefficient of the optical path $W = dn/dT + (n-1)\alpha$ was measured in this study at 1064 nm in the O-cut Nd:KGW crystal for $\boldsymbol{E} \perp N_m$ by the beam deviation method [28] under the homogeneous heating to be $-(7\pm1)\times10^{-6}$ K^{-1}. The W-coefficient for the O-cut Nd:KGW can also be calculated from known values of the thermo-optic coefficient dn_O/dT, index of refraction n_O and thermal expansion α_O. In general, the index of refraction $n(\boldsymbol{E} \perp N_m)$ of a KGW crystal cut for light propagation in the N_p-N_g plane can be calculated as [29]:

$$n(E \perp N_m) = \frac{n_g n_p}{(n_g^2\cos^2\varphi + n_p^2\sin^2\varphi)^{1/2}} \quad (2),$$

with the dn/dT $(\boldsymbol{E} \perp N_m)$ being, after differentiation:

$$\frac{dn}{dT}(E \perp N_m) = \frac{dn_g}{dT}\frac{n^3}{n_g^3}\sin^2\varphi + \frac{dn_p}{dT}\frac{n^3}{n_p^3}\cos^2\varphi \quad (3),$$

where n_g (n_p) and dn_g/dT (dn_p/dT) are the indices of refraction and thermo-optic coefficients, respectively, for $\boldsymbol{E} \parallel N_g$ (N_p), and φ is the angle between the N_g axis and the direction of light propagation in the N_p-N_g plane (φ = 43º in KGW crystal cut along the optical axis). The set of thermo-optical parameters of Nd:KGW at 1 μm is summarised in table 2. The index of refraction in the *O*-cut crystal does not depend on polarisation, i.e. $n_O(\boldsymbol{E}\perp N_m)=n_m=2.01$ at 1067 nm [30] at φ = 43º. The thermo-optic coefficient dn_O/dT does depend on polarisation due to the different physical nature of these dependencies [31-33]. The value of the thermal expansion α_O along the optical axis can be calculated from the following expression [21]:

$$\alpha_O = \alpha_g \cos^2\varphi + \alpha_p \sin^2\varphi \quad (4),$$

where α_g and α_p are the thermal expansion coefficients along the *g* and *p* axes (see table 2 for values). The thermo-optic and thermal expansion coefficients calculated from eqs. (3) and (4) of the *O*-cut Nd:KGW at 1067 nm are shown in table 2. Therefore, the thermal coefficients of the optical path along the optical axis in Nd:KGW crystal are:

$$W_O(E \perp N_m) = \frac{dn_O}{dT}(E \perp N_m) + [n_m - 1]\alpha_O = -6.7\times10^{-6}\,K^{-1} \text{ and}$$
$$W_O(E \,//\, N_m) = \frac{dn_m}{dT} + [n_m - 1]\alpha_O = -1.7\times10^{-6}\,K^{-1}.$$

The calculated value of $W_O(\boldsymbol{E}\perp N_m)$ is in good agreement with the one measured in this study. Unfortunately, due to thermal fracture of the *O*-cut crystal, the measurements of the *W* factor for $\boldsymbol{E} \parallel N_m$ could not been performed and compared with the calculated value, but we believe our calculations are likely to agree well with experiment.

Thus, from eq. (1) it is possible to evaluate the contribution of photo-elastic effect P_{PE} to the overall thermally-induced refraction in diode-pumped Nd:KGW without use of the corresponding photo-elastic coefficients, p_{ijkl}. This is done for the diode-pumped anisotropic crystal for the first time, to our knowledge. The results are summarized in table 3. Here three principal contributions are collected, namely *dn/dT*, P_{PE} and Q_{dist}, together with the overall value of Δ. It should be noted from our results that the photo-elastic contribution increases for both meridional planes A and B as the crystal orientation (cut) changes counter-clockwise from being along N_g to along N_p axis (see figure 1). In N_g- and *O*-cut crystals the maximum (minimum) photo-elastic effect is observed along the direction with the maximum (minimum) value of thermal expansion coefficient α. In contrast, for the N_p-cut Nd:KGW the maximum (minimum) photo-elastic effect is observed along the direction with the minimum (maximum) value of thermal expansion coefficient α (see table 2 for the values of $\alpha_{max,\,min}$ and figure 5 for orientation of thermal expansion axes for each crystal cut). In general, the photo-elastic coefficient is determined by the net action of stress (which is in general a tensor in KGW) and thermal expansion [34], and one should not expect a direct relation between the latter and the value of photo-elastic effect.

The values of P_{PE} term, to the best of our knowledge, have never been reported previously for any crystal orientation of Nd:KGW. For the N_p-cut Nd:KGdW crystal, P_{PE} is positive and comparable in absolute value with *dn/dT*. As a result, the optical power of thermal lens is determined by the opposite action of temperature- and stress-dependent variation of the refractive index. This leads to different signs of the thermal lens for rays lying in principal meridional planes. Substantial difference of P_{PE} values for these planes determines the large astigmatism of thermal lens. The impact of the Q_{dist} term is moderate (20% from |*dn/dT*|), mainly because of a small α_p value (1.7×10^{-6} K^{-1}).

For the *O*-cut crystal the impact of positive Q_{dist} becomes more significant, but still is not enough for the crystal to demonstrate positive thermal lensing along both A and B directions for $\boldsymbol{E}\perp N_m$. In case of $\boldsymbol{E}\parallel N_m$ the net effect of *dn/dT* and Q_{dist} results in a relatively small value of the thermal coefficient of -1.7×10^{-6} K^{-1}. However, the photo-elastic effect in general case should be different for different polari-

sations of light [16, 18]; therefore the values previously calculated for $\boldsymbol{E}\perp N_m$ will not be valid for $\boldsymbol{E}\|N_m$ and, strictly speaking, not only the value, but even the sign of the lens cannot be predicted from the data available in this study. However, our measurements of thermal lens in the *O*-cut Nd:KGW crystal in $\boldsymbol{E}\|N_m$ configuration under the flash-lamp pumping shows that it is positive along direction A and negative along B direction [15]. This allows us to estimate the maximum and minimum values of the photo-elastic contribution to thermal lens (see Table 3) under the current pump conditions.

For the N_g-cut crystal, photo-elastic effect also results in an increase of refractive index ($P_{PE} > 0$). However, the absolute value of P_{PE} is small (compared with the dn/dT and especially the Q_{dist} terms). Thus, the optical power of the thermal lens is mainly determined by the dominance of the positive Q_{dist} over the negative dn/dT term, and thermal lens is positive. The small difference between the P_{PE} values for A and B planes leads to small astigmatism.

Reduction of Δ to $dn/dT+(n-1)\alpha$ is acceptable only for N_g-cut Nd:KGdW, but this approach will results in some underestimation of optical power of thermal lens. In contrast, for N_p-cut and *O*-cut crystal, the P_{PE} term cannot be omitted if the thermo-optic effects are to be described correctly.

5. Conclusions

The contribution of photo-elastic effect to the thermal lens in diode-pumped Nd:KGW lasers at 1 μm was calculated based on measurements of the output laser beam distortions for light propagation along the N_g, N_p and optical axes of the crystal for the first time, to the best of our knowledge. The photo-elastic contribution was found to be positive for all studied crystal orientations. It increases when the crystal cut changes counter-clockwise from being along N_g axis to along N_p axis. In the case of an optical axis-oriented Nd:KGW crystal and for light polarization along N_m, the minimum and maximum values of the photo-elastic contribution were evaluated for the positive and negative thermal lens, respectively.

References

[1] Demidovich A A, Shkadarevich A P, Danailov M B, Apai P, Gasmi T, Gribkovskii V P, Kuzmin A N, Ryabtsev G I and Batay L E 1998 *Appl. Phys. B* **67** 11–5.

[2] Boulon G, Metrat G, Muhlstein N, Brenier A, Kokta M R, Kravchik L and Kalisky Y 2003 *Opt. Mater.* **24** 377–83.

[3] Kuleshov N V, Lagatsky A A, Shcherbitsky V G, Mikhailov V P, Heumann E, Jensen T, Diening A and Huber G 1997 *Appl. Phys. B* **64** 409–13.

[4] Kaminskii A A, Pavlyuk A A, Klevtsov P V, Balashov I F, Berenberg V A, Sarkisov S E, Fedorov V A, Petrov M V and Lyubchenko V V 1997 *Inorg. Mater.* **13** 482–3.

[5] Zolotovskaya S A, Savitski V G, Gaponenko M S, Malyarevich A M, Yumashev K V, Demchuk M I, Raaben H, Zhilin A A and Nejezchleb K 2006 *Opt. Mater.* **28** 919–24.

[6] Liu M, Liu J, Li L and Liu S S 2009 *Laser Phys. Lett.* **6** 437–40.

[7] Major A, Langford N, Graf T, Burns D and Ferguson A I 2002 *Opt. Lett.* **27** 1478–80.

[8] Brunner F, Spuhler G I, der Au J A, Krainer L, Morier-Genoud F, Paschotta R, Lichtenstein N, Weiss S, Harder C, Lagatsky A A, Abdolvand A, Kuleshov N V and Keller U 2000 *Opt. Lett.* **25** 1119–21.

[9] Yumashev K V, Savitski V G, Kuleshov N V, Pavlyuk A A, Molotkov D D and Protasenya A L 2007 *Appl. Phys. B* **89** 39–43.

[10] Loiko P A, Kisel V E, Kondratuk N V, Yumashev K V, Kuleshov N V and Pavlyuk A A 2013 *Opt. Mater.* **35** 582–5.

[11] Savitski V G, Birch R, Fraczek E, Kemp A J, Loiko P A, Yumashev K V, Kuleshov N V and Pavlyuk A A 2013 *Proc. of CLEO/Europe and EQEC 2013* (OSA), P. CA12_12.

[12] Loiko P A, Yumashev K V, Kuleshov N V, Savitski V G, Calvez S, Burns D and Pavlyuk A A 2009 *Opt. Expr.* **17** 23536–43.

[13] Hellstrom J, Henricsson H, Pasiskevicius V, Bunting U and Haussmann D 2007 *Opt. Lett.* **32** 2783–5.

[14] Abdolvand A, Wilcox K G, Kalkandjiev T K and Rafailov E U 2010 *Opt. Express* **18** 2753–9.

[15] Loiko P A, Yumashev K V, Kuleshov N V and Pavlyuk A A 2012 *Appl. Phys. B.* **106** 881–6.

[16] Loiko P A, Yumashev K V, Kuleshov N V and Pavlyuk A A 2010 *Appl. Opt.* **49** 6651–9.

[17] Hamilton W R 1833 Trans. R. Irish Acad. **17** 1-144 (1833).

[18] Zelenogorskii V V and Khazanov E A 2010 *Quantum Electron.* **40** 40–4.

[19] Loiko P A, Yumashev K V, Kuleshov N V and Pavlyuk A A 2012 *Appl. Phys. B* **106** 663–8.

[20] Hodgson N and Weber H 2005 *Laser Resonators and Beam Propagation. Fundamentals, Advanced Concepts, Applications* (Springer, New York).

[21] Loiko P A, Yumashev K V, Kuleshov N V, Rachkovskaya G E and Pavlyuk A A 2011 *Opt. Mater.* **34** 23–6.

[22] Koechner W 2006 *Solid-State Laser Engineering* (Springer, New York).

[23] Chenais S, Druon F, Forget S, Balembois F and Georges P 2006 *Prog. Quantum Electron.* **30** 89–153.

[24] Mazur M M, Velikovskii D Y, Kuznetsov F A, Mazur L I, Pavlyuk A A, Pozhar V E and Pustovoit V I 2012 *Acoustical Physics* **58** 658–65.

[25] Biswal S, O'Connor S P and Bowman S R 2005 *Appl. Opt.* **44** 3093–7.

[26] Mochalov I V 1997 *Opt. Eng.* **36** 1660–9.

[27] Silvestre O, Grau J, Pujol M C, Massons J, Aguiló M, Díaz F, Borowiec M T, Szewczyk A, Gutowska M U, Massot M, Salazar A and Petrov V 2008 *Opt. Expr.* **16** 5022–34.

[28] Vatnik S, Pujol M C, Carvajal J J, Mateos X, Aguiló M, Díaz F and Petrov V 2009 *Appl. Phys. B* **95** 653–6.

[29] Hernández-Rodríguez C and Fragoso-López A B 2014 *Opt. & Laser Techn.* **55** 1–5.

[30] Pujol M C, Rico M, Zaldo C, Sole R, Nikolov V, Solans X, Aguilo M and Diaz F 1999 *Appl. Phys. B* **68** 187–97.

[31] Antoncik E 1956 *Cechoslovackij fiziceskij zurnal* **6** 209–16.

[32] Tsay Y F, Bendow B and Mitra S S 1973 *Phys. Rev. B* **8** 2688–96.

[33] Ghosh G and Palik E 1998 *Handbook of thermo-optic coefficients of optical materials with applications* (Academic Press, San Diego).

[34] Nye J F 1985 *Physical Properties of Crystals* (Clarendon Press, Oxford).

[35] Loiko P A, Yumashev K V, Kuleshov N V, Rachkovskaya G E and Pavlyuk A A 2011 *Opt. Mater.* **33** 1688–94.

Table 1. Parameters of thermal lens for Nd:$KGd(WO_4)_2$ crystals at 1 μm

Parameter		Crystal cut		
		N_p-cut	O-cut	N_g-cut
$M = dD/dP_{abs}$ (ω_p=180 μm), [m^{-1}/W]	along A	+0.57	+0.72	+2.35
	along B	–1.03	–0.92	+2.18
$S = M_A – M_B$, [m^{-1}/W]		+1.60	+1.64	+0.17

Table 2. Thermo-optical parameters of Nd:KGW crystal at 1 μm (corresponding references are shown in square brackets, * denotes results obtained in this paper).

cut	n [29]		dn/dT, 10^{-6} K^{-1} [35]		α, 10^{-6} K^{-1} [20]			κ, W/(mK) [26]
	$\boldsymbol{E}\|\|N_m$	$\boldsymbol{E}\perp N_m$	$\boldsymbol{E}\|\|N_m$	$\boldsymbol{E}\perp N_m$	α	α_{max}	α_{min}	
N_p		2.06 ($\boldsymbol{E}\|\|N_g$)		-17.7 ($\boldsymbol{E}\|\|N_g$)	1.7	20.6	7.6	3.4
O	2.01	2.01	-11.7	-16.6*	9.8*	14.2*	5.9*	2.7*
N_g		1.98 ($\boldsymbol{E}\|\|N_p$)		-15.9 ($\boldsymbol{E}\|\|N_p$)	16.9	11.3	1.7	2.9

Table 3. Contribution of photo-elastic effect to thermal lens optical power in diode-pumped Nd:$KGd(WO_4)_2$

Crystal	Contribution to optical power of thermal lens, [10^{-6} K^{-1}]			Δ, [10^{-6} K^{-1}]
	dn/dT	P_{PE}	Q_{dist}	
N_p-cut, $\boldsymbol{E}\|\|N_m$	–11.7	+11.2 (A) +7.3 (B)	+1.8	+1.3 (A) –2.6 (B)
O-cut, $\boldsymbol{E}\perp N_m$	–16.6	+8.5 (A) +4.4 (B)	+10.0	+1.9 (A) –2.2 (B)
$\boldsymbol{E}\|\|N_m$	–11.7	>+1.7 (A) <+1.7 (B)	+10.0	Positive (A) [15] Negative (B) [15]
N_g-cut, $\boldsymbol{E}\|\|N_m$	–11.7	+0.6 (A) +0.2 (B)	+17.0	+5.9 (A) +5.5 (B)

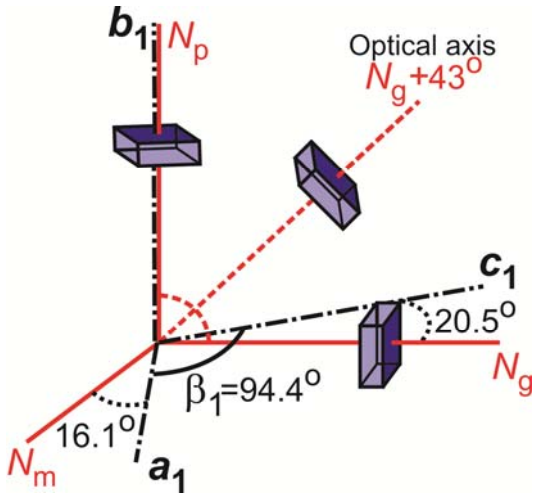

Figure 1. Orientation of studied Nd:$KGd(WO_4)_2$ laser crystals with respect to axes of optical indicatrix (N_p, N_m, N_g) and crystallographic axes ($\boldsymbol{a}_1$, $\boldsymbol{b}_1$, $\boldsymbol{c}_1$ – I2/c).

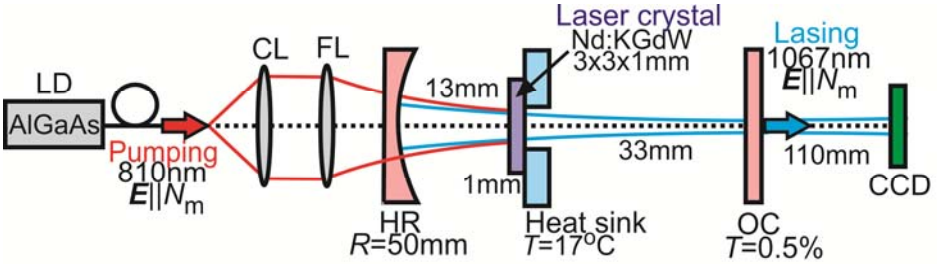

Figure 2 Experimental set-up for thermal lens measurements in Nd:$KGd(WO_4)_2$ laser crystal.

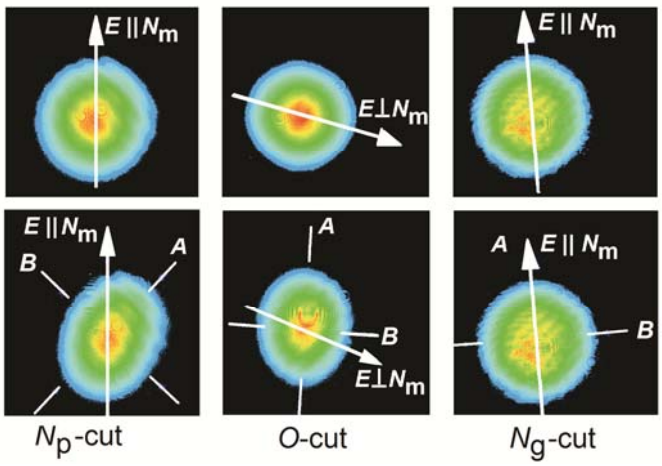

Figure 3 Spatial profiles of the output beam of a diode-pumped Nd:$KGd(WO_4)_2$ laser based on N_p-, N_g- and *O*-cut crystals; *upper* and *lower* images correspond to low and high pump level.

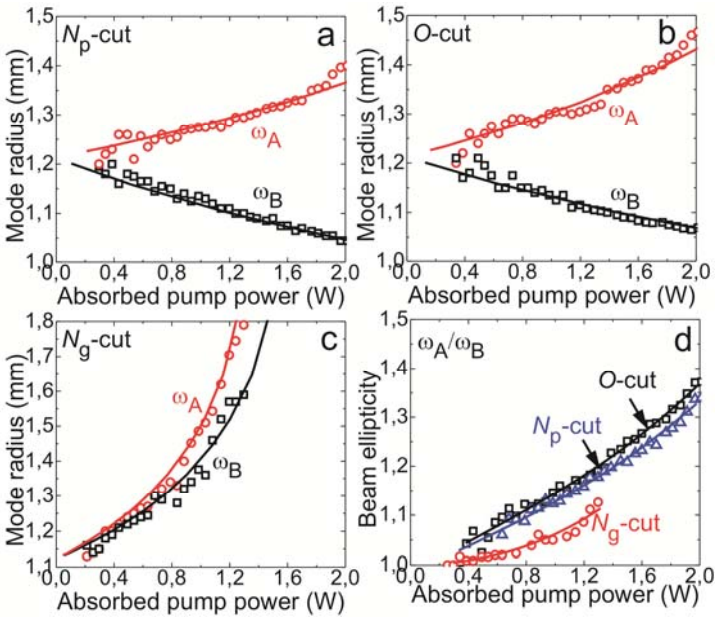

Figure 4 Radii of TEM_{00} laser mode, $\omega_{A(B)}$, as a function of the absorbed pump power for N_p-cut (a), O-cut (b) and N_g-cut (c) Nd:$KGd(WO_4)_2$ crystals; (d) beam ellipticity ω_A/ω_B.

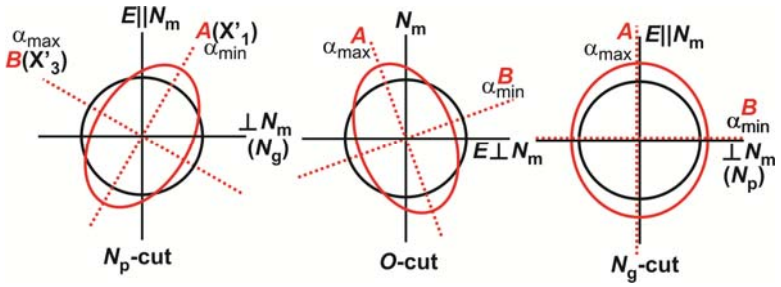

Figure 5 Distortion of output beam of Nd:$KGd(WO_4)_2$ laser due to influence of thermal lens: black *circles* and red *ellipses* correspond to beam profiles at low and high pump levels, *dotted* lines correspond to principal meridional planes (A and B directions).

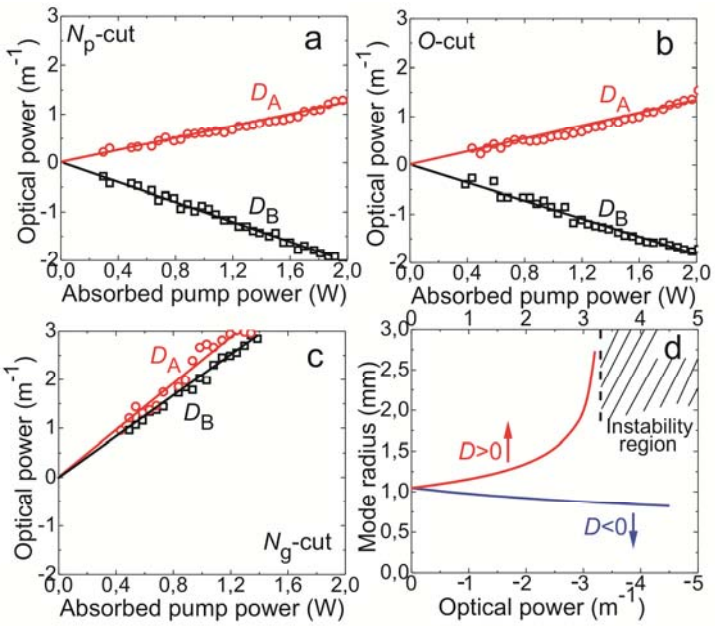

Figure 6 Optical power of thermal lens along principal meridional planes, $D_{A(B)}$, as a function of the absorbed pump power for N_p- (a), O- (b) and N_g-cut (c) Nd:$KGd(WO_4)_2$ crystals; (d) ABCD-modelling of output mode of Nd:$KGd(WO_4)_2$ laser.